



## Effect of Inlet Pressure on the Polyurethane Spray Nozzle for Soil Cracking Improvement: Simulations using CFD Method

Tasnim Zakepeli<sup>1</sup>, Nik Normunira Mat Hassan<sup>1,\*</sup>, Nur Afzanizam Samiran<sup>2</sup>, Anika Zafiah Mohd Rus<sup>3</sup>, Noraini Marsi<sup>1</sup>, Tuan Noor Hasanah Tuan Ismail<sup>1</sup>, Mohd Ridzuan Mohd Jamir<sup>4</sup>, Siti Nur Azila Khalid<sup>5</sup>, Muhamad Iqbal Aiman Mohd Azman<sup>6</sup>

<sup>1</sup> Faculty of Engineering Technology, Universiti Tun Hussein Onn Malaysia, Pagoh Higher Education Hub, 84600 Pagoh, Muar, Johor, Malaysia

<sup>2</sup> Faculty of Mechanical and Manufacturing Engineering, Universiti Tun Hussein Onn Malaysia, Pagoh Higher Education Hub, 84600 Pagoh, Muar, Johor, Malaysia

<sup>3</sup> Sustainable Polymer Engineering, Advance Manufacturing and Material Center (AMMC), Faculty of Mechanical and Manufacturing Engineering, Universiti Tun Hussein Onn Malaysia, Jalan Kluang 86400 Batu Pahat, Johor, Malaysia

<sup>4</sup> Faculty of Mechanical Engineering Technology, Universiti Malaysia Perlis, Pauh Putra Campus, 02600 Arau, Perlis, Malaysia

<sup>5</sup> JKR State Mechanical Engineering Branch, Jalan Sri Kemunting 2, Tanah Putih, 25100 Kuantan, Pahang, Malaysia

<sup>6</sup> Ideal Quality Sdn. Bhd, Kawasan Perindustrian Meru Selatan, 41050 Klang, Selangor, Malaysia

### ARTICLE INFO

#### Article history:

Received 2 November 2023

Received in revised form 6 December 2023

Accepted 10 January 2024

Available online 31 July 2024

#### Keywords:

PU spray nozzle; pressure inlet; velocity spray

### ABSTRACT

Rigid spray polyurethane (RSPU) was commercially used as an injection in crack walls or soil surfaces to enhance material performance, increase lifetime, and save operating costs. The limitation of the RSPU nozzle was reported as easily clogging when sprayed out to the insulation and crack surface area and the finished product was less aesthetically pleasing. In this study, the RSPU nozzle of flat fan nozzle, 180° angle (Design A), Hollow cone nozzle, 60° angle (Design B), and Full cone nozzle, 90° angle (Design C) were prepared by using the SOLIDWORKS software. The effect of different pressures for RSPU nozzle design at the ranges of 4MPa, 5MPa, and 6MPa was examined by ANSYS FLUENT software. The velocity of the outer spray nozzle shows a significant increase with increasing inlet pressure of the RSPU nozzle. The results reveal that the highest velocity of RSPU was obtained at the Hollow cone nozzle (Design B) as compared to (Flat fan nozzle) Design A and (Full cone nozzle) Design C at 394.249 m/s at 4MPa, 442.327 m/s at 5MPa and 485.37 m/s at 6MPa, respectively. The distribution droplet area shows the Design B spray formation had wider area coverage at 60° and exhibited that the injection nozzle spray was scattered and uniform at 6MPa. RSPU shows the velocity increased, distribution droplet increased, and output volume spray was decreased at the increasing of injection pressure. Hence, in this study was suggested that the size of RSPU nozzle design must be made at the ranges of 60° to 90° of outlet nozzle to obtain a good RSPU area. In conclusion, design B is the most effective for RSPU nozzle and is useful in injection cracking and insulation materials applications.

\* Corresponding author.

E-mail address: [normunira@uthm.edu.my](mailto:normunira@uthm.edu.my) (Nik Normunira Mat Hassan)

<https://doi.org/10.37934/cfdl.16.12.5971>

## 1. Introduction

Spray polyurethane (SPU) was commercially used as insulation in industrial equipment in pipes, tanks, and ducting to enhance energy efficiency, increase lifetime, and save operating costs. It may also be used to seal and protect surfaces against corrosion, wear and tear, and other sorts of damage, such as those found on machinery and equipment. SPU is one of the most popular methods of insulation in the manufacturing and geotechnical industry. SPU is utilized in a range of manufacturing applications, including insulation for industrial equipment and facilities, product sealing and coating, and surface protection. The previous research reported that the use of the cold spray process for depositing a range of powder particles including metals, polymers, composites, and ceramics on diverse substrates since its first application as a coating technology more than 30 years ago [1].

Most of the SPU materials are the rigid polyurethane (PU) foams. These rigid polyurethane foams have excellent thermal insulation, low density, high specific strength, good dimensional stability, and adhesion strength as well as aging resistance, which makes them attractive high-performance materials for offering numerous applications [2]. SPU is a very effective thermal insulation material that is utilized in a variety of commercial construction applications such as internal and external wall insulation, basement and ceiling insulation, and floor and flat roof insulation [3]. SPU is a stiff foam that is currently employed in residential and commercial structures as wall insulation [4]. SPU insulation has two components, component 'A' as isocyanate and component 'B' as polyol. It expands many times its volume and solidifies in seconds sealing the wall [4].

However, in SPU the part of spray nozzles has been utilized in a range of industrial applications such as spray blasting, spray cooling, spray coating, and agricultural spray, and they come in single-spray, twin-spray, and multi-spray forms [5]. SPU is a very effective thermal insulation material that has had significant market expansion over the last decade. SPU is also used as spray-applied insulation that has the ability to decrease air infiltration through cracks, seams, and joints [6]. PU spraying consists of projecting the PU into a surface or a cavity. It is normally used for insulation layers on flat surfaces such as roofs [7].

In current practice, on-site applications, SPU exhibited the issues with two-component PU foam systems in practice on-site used in the manufacturing sector. The main problems reported in the spray application of PU, caused by the finished product depend primarily on the proper application and properties of the in-place foam. This is also due to foam hardens in a two-component system in a very short period of time via chemical reaction with the reaction of polymerization isocyanate hardener, the guns must be cleaned immediately after use [8].

SPU nozzle is commonly clogged when PU flow particles move through the nozzle, the PU liquid occasionally collides with the nozzle's inner wall, causing particle-to-nozzle wall bonding and, eventually promoting the nozzle blockage [9]. This is due to the ability of PU flow to give effect to the outlet nozzle in order to produce aesthetically pleasing products and achieve faster cycle times and higher yields, fundamentally the processing techniques are frequently compromised, resulting in unexpected failures [10].

Hence, to prevent the clogging in outer nozzle issues, this study focused attention on studying the maximum value of the velocity and pressure applied on spray nozzles used to apply polyurethane foams directly to the rigid surface and at the same time to improve the surface finishing product. This SPU nozzle selection is critically needed to prevent spray drift and improve the efficiency of the insulation repair application. Hence, the objectives of this study were to examine the effect of pressure and velocity on the SPU nozzle at three different designs with the outlet nozzle angle 60°, 90°, and 180° with the injection pressure of 4MPa, 5MPa, and 6MPa by using the CFD method.

## 2. Methodology

### 2.1 Geometry Development

The purpose of this study was to examine how varying pressures affected the flowability of a rigid PU spray nozzle that had three different sizes of nozzles design at different angles of 60°, 90°, and 180° as referred to in Figure 1. The rigid PU spray nozzle was designed based on the developed model from the previous research by Barman *et al.*, [11]. The different types of rigid PU spray nozzle designs were set as a baseline on the length dimension of 20mm. Whereas the modified design involved the size of the rigid PU spray nozzle with a shapes design flat fan (Design A), hollow cone (Design B), and full cone (Design C). The study by Barman *et al.*, [11] used a cylindrical shape with a diameter of 47.1mm. The rigid PU spray nozzle size was created using the usual arrangement depicted in Figure 1 and the dimension of the spray nozzle in Table 1.

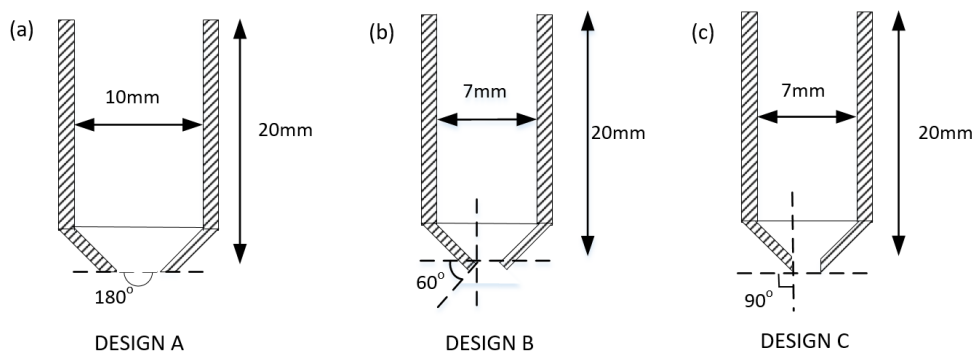


**Fig. 1.** Three types of rigid PU spray nozzle (a) Nozzle design A (b) Nozzle design B and (c) Nozzle design C

**Table 1**  
 Dimensions of the spray nozzle

Parameter nozzle	Angle (°)	Diameter (mm)	Length (mm)
Design A	180	10	20
Design B	60	7	20
Design C	90	7	20

### 2.2 Boundary Condition

The model's area restrictions are defined in boundary conditions as shown in Figure 2. In this model, there are three boundary conditions which are inlet flow, outlet flow, and wall. In this analysis, the water fluid domain was selected and represents the rigid PU fluid spray and was set to collect at the inlet selection before being injected into the chamber. The next boundary condition is the injection of rigid PU fluid spray into the chamber through the outflow. Finally, the last boundary condition is the wall, which has no motion. As a result, the rigid PU spray nozzle and chamber walls can be declared stationary as shown in Table 2.

**Table 2**  
 The parameters used throughout the whole simulation

Nozzle design	Injection inlet pressure (MPa)	Solver	Time	Viscous model	Fluid material
Design A	4, 5 & 6	Pressured based	Steady	K-epsilon	Polyurethane
Design B	4, 5 & 6				
Design C	4, 5 & 6				

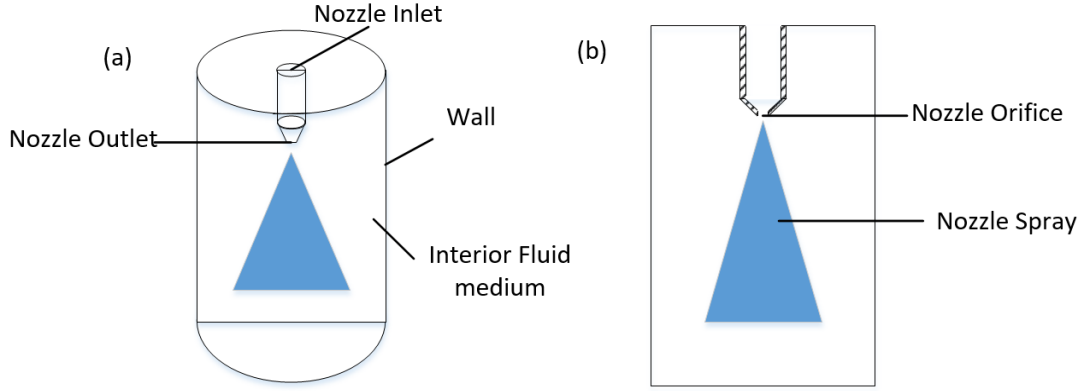


**Fig. 2.** (a) Boundary conditions in 3-Dimensional view (b) Location of nozzle orifice and spray (sectional view)

### 2.3 Governing Equation

CFD includes the numerical solution of conservation equations. The Reynolds-averaged Navier-Stokes (RANS) equations were simultaneously solved using the finite control volume with cylindrical coordinates was applied. The governing equation in the simulation study included mass conservation and conservation of momentum in Z, R, and  $\theta$  direction as formulated in Eq. (1), Eq. (2) and Eq. (3) respectively [12,13].

In Z-direction

$$\rho \left( \frac{\partial U}{\partial t} + U \frac{\partial U}{\partial z} + V \frac{\partial U}{\partial r} + \frac{W}{r} \frac{\partial U}{\partial \theta} \right) = -\frac{\partial p}{\partial r} + \left[ \frac{1}{r} \frac{\partial}{\partial r} (r \tau_{rz}) + \frac{1}{r} \frac{\partial}{\partial \theta} \tau_{\theta z} + \frac{\partial}{\partial z} \tau_{zz} \right] + \rho F_z \quad (1)$$

In R-direction

$$\rho \left( \frac{\partial V}{\partial t} + U \frac{\partial V}{\partial z} + V \frac{\partial V}{\partial r} + \frac{W}{r} \frac{\partial V}{\partial \theta} - \frac{w^2}{r} \right) = -\frac{\partial p}{\partial r} + \left[ \frac{1}{r} \frac{\partial}{\partial r} (r \tau_{rr}) + \frac{1}{r} \frac{\partial}{\partial \theta} \tau_{\theta r} + \frac{\partial}{\partial z} \tau_{zr} - \frac{\tau_{\theta\theta}}{r} \right] + \rho F_r \quad (2)$$

In  $\theta$ -direction

$$\rho \left( \frac{\partial W}{\partial t} + V \frac{\partial W}{\partial z} + \frac{W}{r} \frac{\partial W}{\partial \theta} + \frac{WV}{r} + U \frac{\partial W}{\partial z} \right) = -\frac{1}{r} \frac{\partial p}{\partial \theta} + \left[ \frac{1}{r^2} \frac{\partial}{\partial r} (r^2 \tau_{r\theta}) + \frac{1}{r} \frac{\partial}{\partial \theta} \tau_{\theta\theta} + \frac{\partial}{\partial z} \tau_{z\theta} + \frac{\tau_{\theta r} - \tau_{r\theta}}{r} \right] + \rho F_\theta \quad (3)$$

Where  $\rho$  is the density at the point considered in the continuum (for which the continuity equation holds),  $\tau$  is the stress tensor, and  $\rho F$  contains all of the body forces per unit mass (often simply gravitational acceleration).

### 2.4 Grid Development

The meshing construction involved the breakdown process of domain into thousand or more shapes each representing an element of the component. The meshing process for the present study was developed for each component domain in the rigid PU spray nozzle as depicted in Figure 3. The mesh type of solid mesh has been applied and every core surface and volume meshing were used in this meshing model. The element size for a mesh-based curvature is numerically approximated by the average number of elements that fit inside a hypothetical circle, while taking into account the user-specified minimum and maximum element sizes [14]. Table 3 shows the generated meshing properties of the present model. The total number of elements generated was 2161069 for design A, 123699 for design B and 128261 for design C, respectively.



**Fig. 3.** The result of the generated of mesh PU spray nozzle model

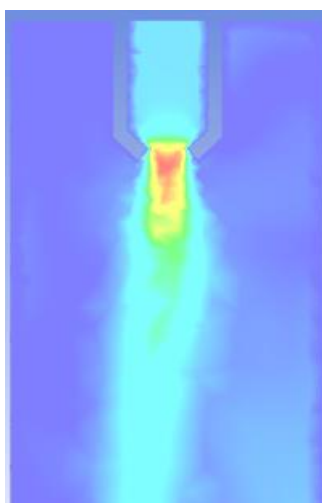
**Table 3**

Mesh property			
Parameter nozzle	Mesh type	Total nodes	Total element
Design A	Solid mesh	400660	2161069
Design B	Solid mesh	24985	123699
Design C	Solid mesh	123699	128261

### 3. Results

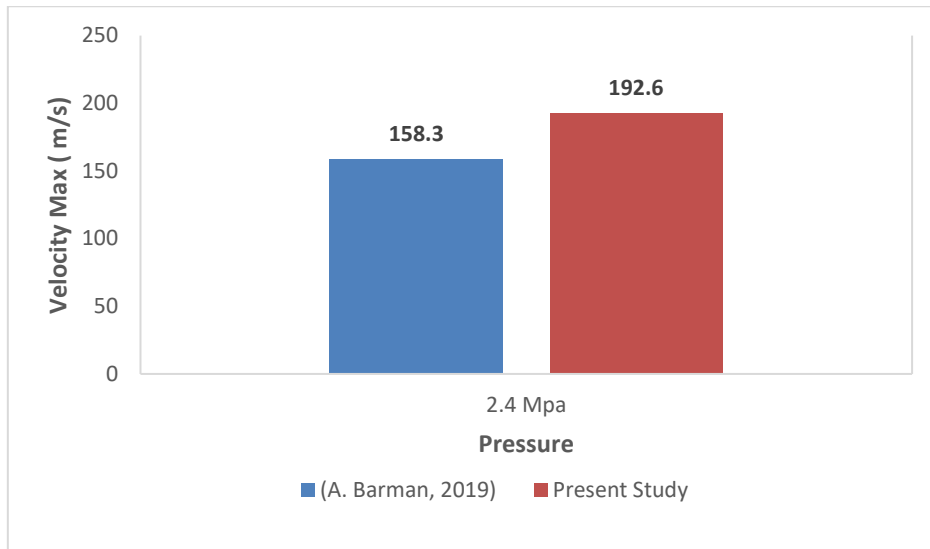
#### 3.1 Model Validations

Figure 4 shows the distribution of the velocity magnitude model of the simulation generated with a water spray nozzle under an inlet pressure of 24 bar using the ANSYS simulation. The present results were validated with the previous study as shown in Figure 5. The created domain is cylindrical in shape with a radius of 23.55 mm and a length of 60 mm. Figure 5 shows that the present study is in good agreement with the Barmen, *et al.*, [11]. According to Barmen, *et.al* [11] mentioned that the nature of the spray produced at the nozzle exit is a hollow cone spray and the maximum velocity of exit at the nozzle outlet is found to be in the range of 55 - 60 m/s.



**Fig. 4.** The distribution of velocity in simulation nozzle chamber

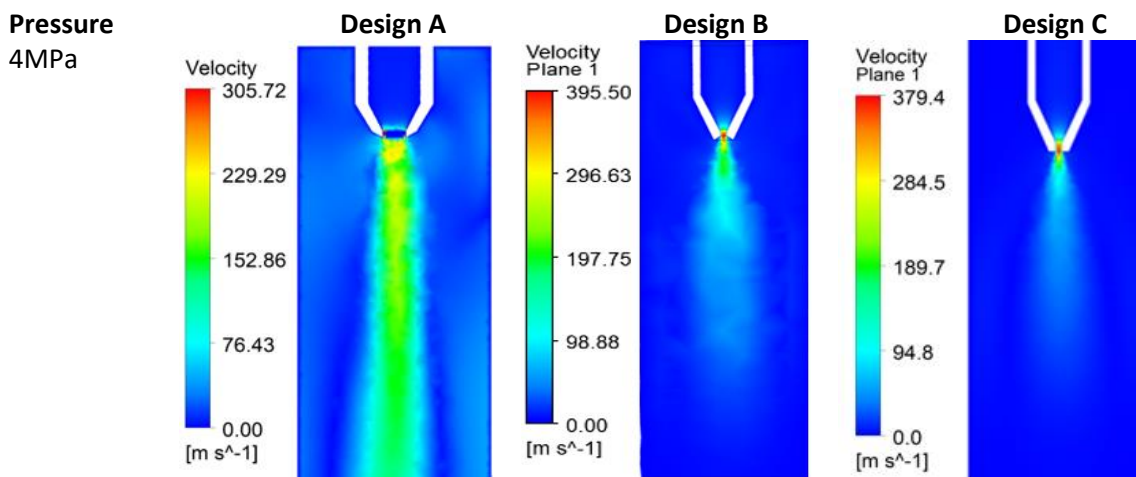
The present results showed a deviated value of few percentages with Barmen, *et al.*, [11] at the position of the same injection pressure. The deviation seems to be caused by the different fluid properties used on the inlet of the simulation chamber was 158.3 m/s for Barmen, *et al.*, [11] and 192.6 m/s for the present result. The percentage error was 17.8% which is below 20%. The value of percentage error was close to the previous study from Joanna *et al.*, [15] which also performed spray injection simulations and suggested that 18% was the relative error between the experimental with the mathematical model. Hence, this evidently was considered that our percentage value is acceptable to be used for simulation in this study [15].



**Fig. 5.** Comparison of simulation result between previous study by Barman [11] and present study

### 3.2 Effect of Velocity at a Different Inlet Pressure of PU Spray Nozzle

Figure 6 illustrate the velocity contours at different inlet pressure of 4MPa, 5MPa, and 6MPa of spray nozzle Design A, Design B, and Design C.



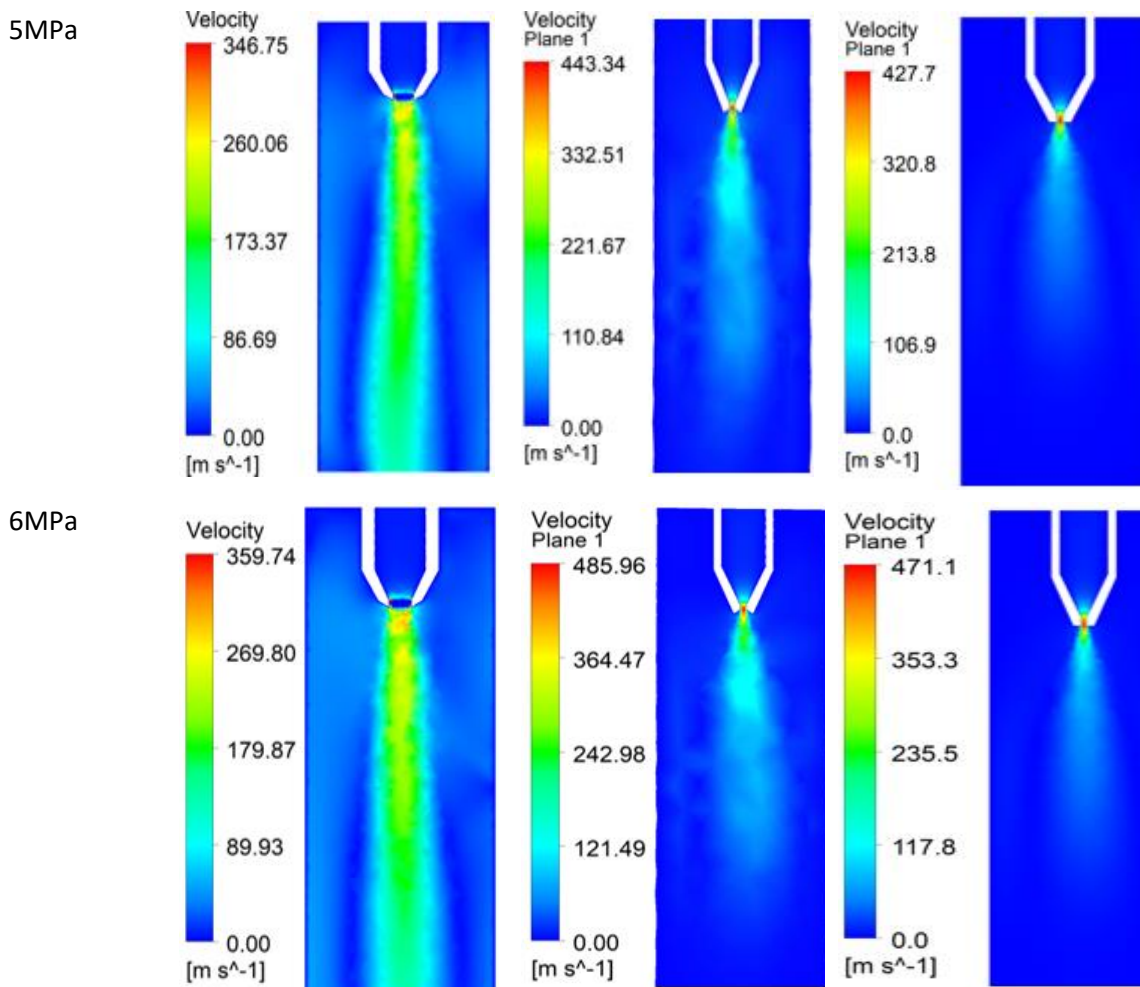


**Fig. 6.** Velocity contours at 4MPa, 5MPa, and 6MPa of different rigid PU spray nozzle of Design A, Design B, and Design C

From the observation, the volume of the rigid PU fluid spray nozzle from the outlet nozzle spray shows the distribution area of injection was lowest at design C followed by design B and design A. However, at Design B with  $60^\circ$  outlet nozzle angle gives a uniform distribution flow and long-distance flow as compared to Design C with  $90^\circ$  outlet nozzle angle. This is may due to the effect of the different sizes of the outer spray nozzle design angle which is at the range  $180^\circ$  (Design A),  $60^\circ$  (Design B), and  $90^\circ$  (Design C) distribution direction respectively.

The velocity of rigid PU fluid spray result of this research study was a similar trend to previous research by scholar [16]. This previous research mentioned that the higher spray velocity results of smaller droplet size give more uniform droplet distribution and a more consistent and uniform spray pattern. However, the value of velocity results of this simulation is different from previous research which is  $60 \text{ m/s}$  as the material and boundary condition used for this simulation may be different than the previous work.

Moreover, the relationship between rigid PU spray velocity and the spray formation was complex and influenced by several factors. As the velocity increases, droplets become smaller, and droplet distribution becomes more uniform, which improves the overall surface finish, but it also increases the chances of overspray and rebound. Therefore, it is important to consider the trade-offs and find the optimal rigid PU spray velocity that balances the benefits and drawbacks for the specific application and manufacturing process.

Figure 7 shows the summary of the maximum velocity of different nozzle designs of Design A, Design B, and Design C at different pressures from 4MPa, 5MPa, and 6MPa, respectively. The result shows the maximum velocity of the spray nozzle significantly increased with increasing inlet pressure. However, the velocity of the distribution droplet also influenced by the nozzle shape which is a different design of the spray nozzle due to smallest spray area gives the good performance of spray fluid distributions. The spray velocity at an inlet pressure of 6MPa, for example, has the maximum value for design A. When the injection pressure is increased, the velocity of the fluid out increases. These suggested that a velocity increase contributed to the volume of fluid that was sprayed out from the spray nozzle when injection pressure increased. So, the PU performance spray may become more efficient with the optimum pressure and angle of spray nozzle.

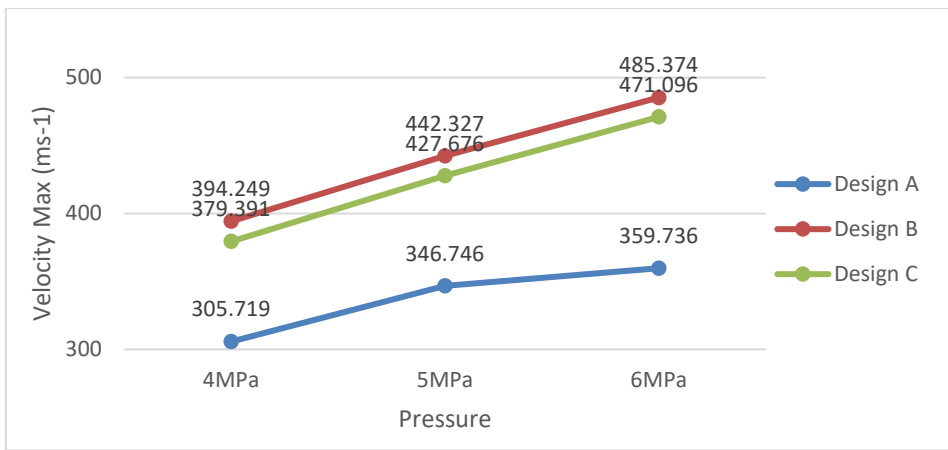


**Fig. 7.** Maximum velocity of different nozzle design of Design A, Design B, and Design C at different pressure from 4MPa, 5MPa, and 6MPa

Overall, the velocity effect on the distribution droplet of the rigid PU fluid spray shows that Design B, with a maximum velocity of 442.327 m/s, would likely produce the smallest droplet size and most uniform droplet distribution. However, it is important to consider other factors such as nozzle geometry, fluid properties, and environmental conditions before determining the best spray nozzle design.

### 3.3 Effect of Formation at Different Injection Pressure of Rigid PU Spray Nozzle

From the study, the volume of rigid PU fluid in a spray-out pattern shows not uniform and scattered droplet distribution at Design A, Design B, and Design C as shown in Figure 8. Based on the pressure effect, the pattern shows with increasing the volume of rigid PU fluid, the droplet distribution also increased with increasing injection pressure of 4MPa, 5MPa, and 6MPa at Design A, Design B, and Design C, respectively. Design B shows a higher volume of rigid polyurethane fluid spray at 4MPa, 5MPa, and 6MPa as compared to Design A and Design C. This is due to the angle of the spray nozzle Design B being 60 degrees gives more direction to inject and spread the rigid polyurethane fluid according to the nozzle shapes and insulation surface areas.

The spray formation of the study was a similar trend to previous research by author [17]. These previous research findings have shown that spray formation is greatly influenced by the nozzle design, fluid properties, and operating conditions. The volume of spray out from the nozzle is affected by the fluid velocity and pressure at the nozzle exit. As the velocity increases, the spray formation of the spray nozzle, also becomes wider, while the droplet size decreases slightly to the spray nozzle design.

Spray formation is a critical aspect of the design and development of spray nozzles. It refers to the way in which fluid is dispersed from a nozzle into droplets or a spray pattern. The volume of spray out from the nozzle is dependent on various factors such as fluid properties, nozzle geometry, and operating conditions. Generally, a higher volume of rigid polyurethane fluid spray at 4MPa, 5MPa, and 6MPa for Design B compared to Design A and Design C. The spray formation and the volume of spray out from the nozzle are closely related and are dependent on several interrelated factors.

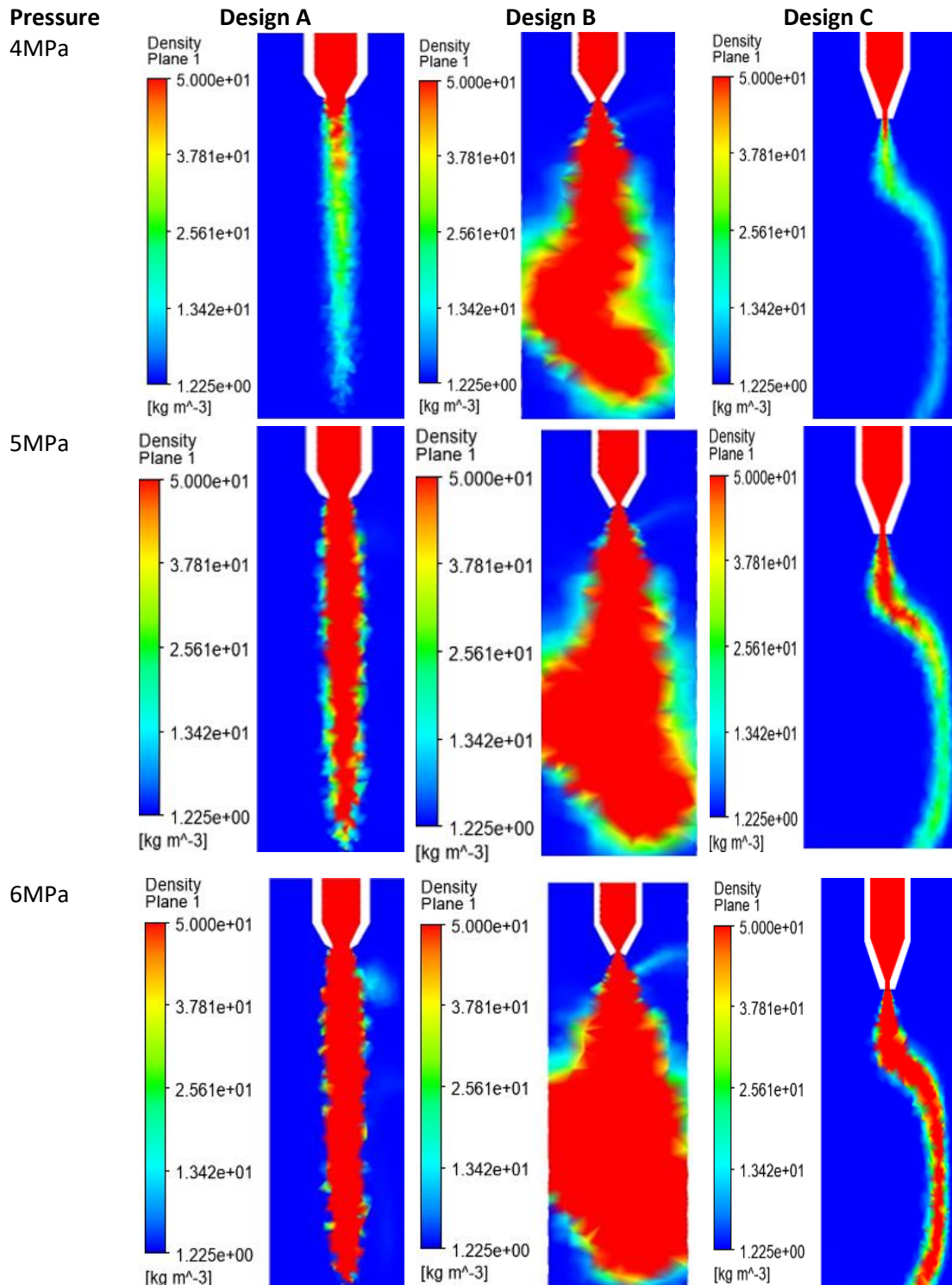


**Fig. 8.** The spray formation contour at 4MPa, 5MPa and 6MPa of 3 different nozzle design which is of Design A, Design B and Design C

### 3.4 Effect of Spray Cone Angle at a Different Injection Pressure of Rigid PU Spray Nozzle

Figure 9 shows the spray cone angle for 4MPa, 5MPa, and 6 MPa pressure of 3 different nozzle designs which are Design A, B, and C. The result uncovers that the spray cone angle of the spray-out pattern shows different outcomes of the spray nozzle design. Design B reached the highest cone angle followed by Design C and Design A. This is may due to various factors, including fluid properties, nozzle geometry, and operating conditions.

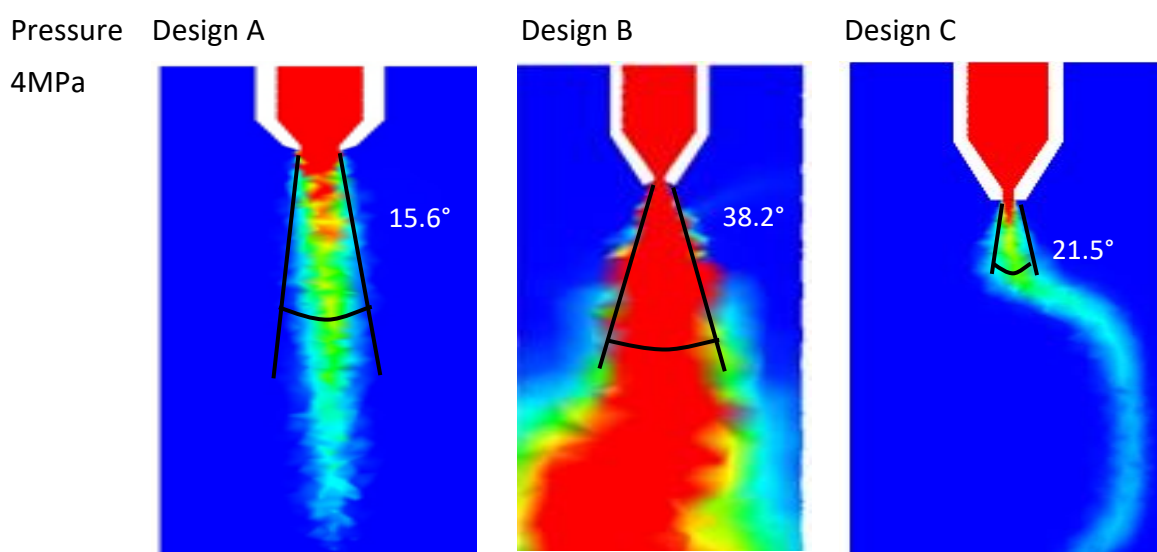
From the previous research, the trend of the result is similar to the [18]. Previous research has shown that the spray cone angle is directly related to the volume of spray out from the nozzle. An increase in the spray cone angle results in a larger volume of rigid polyurethane fluid spray, while a decrease in the spray cone angle leads to a smaller volume of fluid spray. This relationship is due to the relationship between the spray cone angle and the fluid velocity, which directly affects the volume of rigid polyurethane fluid spray.

Table 4 shows the spray cone angle of Design B is the highest at 38.2° at 4MPa, 39.2° at 5MPa, and 39.8° at 6MPa. The spray cone angle and the volume of spray out from the nozzle are closely related, with changes in the spray cone angle resulting in changes in the volume of fluid spray.

**Table 4**  
 The angle of spray nozzle at different inlet pressure

Inlet pressure	4MPa	5MPa	6MPa
Design A Angle (°)	15.6	16.1	16.9
Design B Angle (°)	38.2	39.3	39.8
Design C Angle (°)	21.5	22.2	23.1

The velocity and penetration angle of a new development nozzle exhibited that increasing the pressure of water and air increases the velocity of the water droplet. Hence, changing the ratio of water and air flow rate can considerably increase water droplet velocity and water droplet angle penetration performance [19]. Previous research also reported that airflow velocity measurement of the electrostatic for spray coating application at the pressure from 0.2 to 0.8 MPa and selected in accordance with the established operating spraying condition [20].



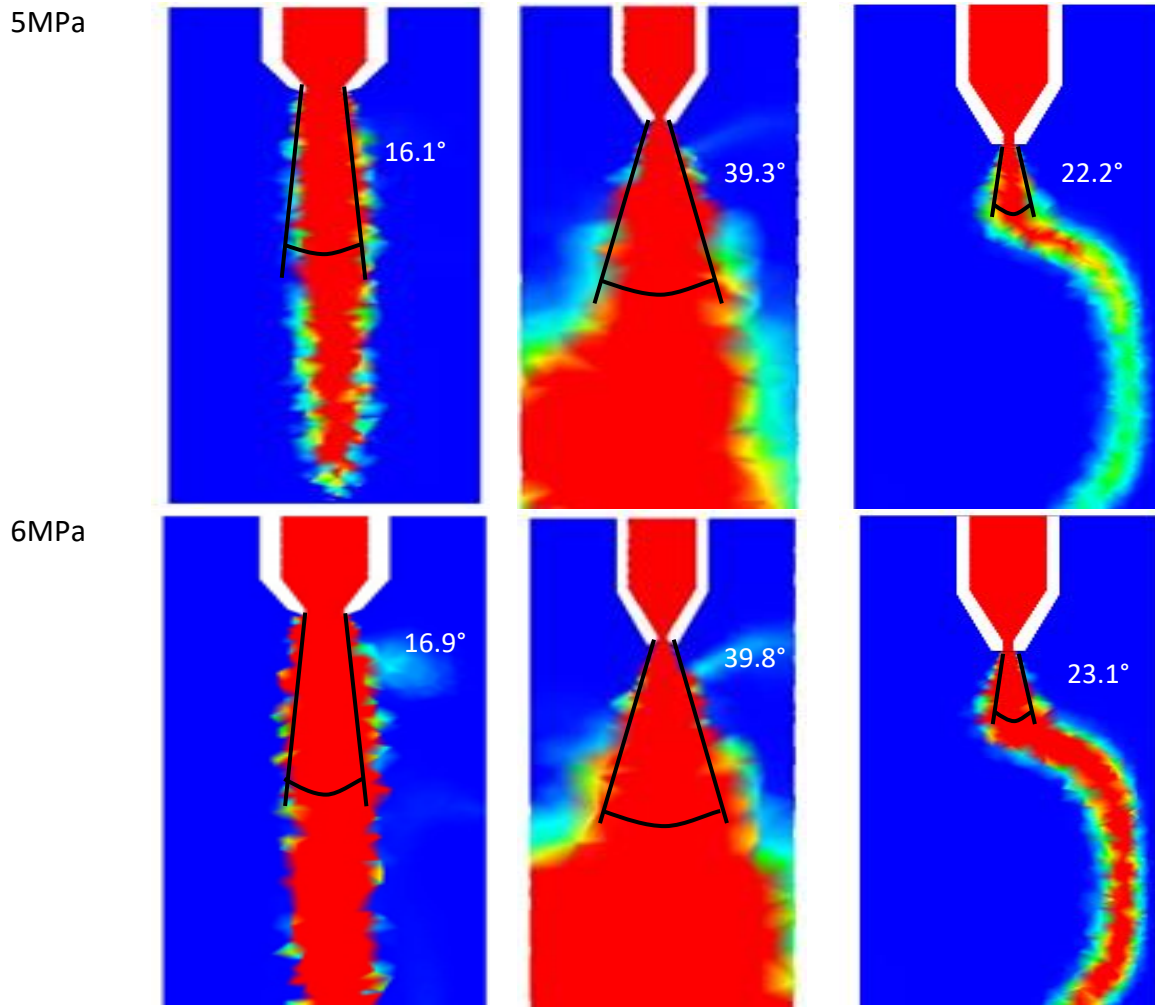


**Fig. 9.** The spray cone angle at 4MPa, 5MPa and 6MPa of 3 different nozzle design which is of Design A, Design B and Design C

#### 4. Conclusions

In conclusion, the objective of this study is to compare the spray nozzle of rigid PU spray nozzle as a function of insulation by using the ANSYS software for insulation materials applications. The results reveal that the highest velocity of rigid PU spray was obtained at Design B with an outer nozzle angle is  $60^\circ$  as compared to Design A and Design C. The velocity of Design B shows 394.249 m/s at 4MPa, 442.327 m/s at 5MPa, and 485.37 m/s at 6MPa, respectively. The distribution droplet area shows the Design B spray formation had wider area coverage at  $60^\circ$  and exhibited that the distribution droplet of the injection nozzle spray was scattered and uniform at 6MPa. This study suggested that the size of rigid PU spray nozzle design must be made at the ranges of  $60^\circ$  until  $90^\circ$  of outlet nozzle to obtain a good spray area. When compared to the other designs, design B is the most efficient in terms of spray velocity, spray formation, and spray cone angle and possibly the most suitable to use in the manufacturing and geotechnic industry to improve the use of SPU and was suggested way to solve the current problem of clogging the outer nozzle during the insulation soil cracking installations.

## Acknowledgment

This research was supported by Ministry of Higher Education (MOHE) through Fundamental Research Grant Scheme (FRGS/1/2022/TK02/UTHM/03/4).

## References

- [1] Khalkhali, Zahra, and Jonathan P. Rothstein. "Characterization of the cold spray deposition of a wide variety of polymeric powders." *Surface and Coatings Technology* 383 (2020): 125251. <https://doi.org/10.1016/j.surfcoat.2019.125251>
- [2] Yang, Rong, Wentian Hu, Liang Xu, Yan Song, and Jinchun Li. "Synthesis, mechanical properties and fire behaviors of rigid polyurethane foam with a reactive flame retardant containing phosphazene and phosphate." *Polymer Degradation and Stability* 122 (2015): 102-109. <https://doi.org/10.1016/j.polymdegradstab.2015.10.007>
- [3] Bello, Anila, Courtney C. Carignan, Yalong Xue, Heather M. Stapleton, and Dhimiter Bello. "Exposure to organophosphate flame retardants in spray polyurethane foam applicators: Role of dermal exposure." *Environment international* 113 (2018): 55-65. <https://doi.org/10.1016/j.envint.2018.01.020>
- [4] Khazabi, Mustafa. *Investigation of biopolyol spray foam insulation modified with natural fibers*. University of Toronto (Canada), 2015.
- [5] Choi, Minsung, Seongyong Eom, Yonmo Sung, Kiyoul Noh, and Gyungmin Choi. "Experimental prediction of multi-nozzle spray characteristics for optimal design in a lead frame etching process." *Journal of Mechanical Science and Technology* 32 (2018): 2127-2139. <https://doi.org/10.1007/s12206-018-0422-3>
- [6] Poppendieck, Dustin, Mengyan Gong, Lisa Ng, Brian Dougherty, Vu Pham, and Stephen M. Zimmerman. "Applicability of spray polyurethane foam ventilation guidelines for do-it-yourself application events." *Building and Environment* 157 (2019): 227-234. <https://doi.org/10.1016/j.buildenv.2019.04.033>
- [7] Gama, Nuno V., Artur Ferreira, and Ana Barros-Timmons. "Polyurethane foams: Past, present, and future." *Materials* 11, no. 10 (2018): 1841. <https://doi.org/10.3390/ma11101841>
- [8] Slutskii, Sergei, and Vitalii Titorov. "Composition of and nozzle for spraying a single-component polyurethane foam." U.S. Patent 10,350,617, issued July 16, 2019.
- [9] Wang, Xudong, Bo Zhang, Jinsheng Lv, and Shuo Yin. "Investigation on the clogging behavior and additional wall cooling for the axial-injection cold spray nozzle." *Journal of Thermal Spray Technology* 24 (2015): 696-701. <https://doi.org/10.1007/s11666-015-0227-1>
- [10] Shakirova, Gulgena, Natalia Romanova, and Lenar Shafigullin. "Analysis of defect causes for rigid PU foam used in the machine building industry." *Materials Today: Proceedings* 19 (2019): 1972-1976. <https://doi.org/10.1016/j.matpr.2019.07.054>
- [11] Barman, A., P. P. Sahoo, and R. Sharma. "A Cfd Based Simulation Model For Design Of Fixed Nozzle." In *7th International Congress on Computational Mechanics and Simulation*, pp. 11-13. 2019.
- [12] Rasool, Adnan AAR, Safaa S. Ahmad, and Faik Hamad. "Effect of impeller type and rotational speed on flow behavior in fully baffled mixing tank." *International Journal of Advanced Research (IJAR)* 5, no. 1 (2017): 1195-1208. <https://doi.org/10.21474/IJAR01/2871>
- [13] Baba, Ahmad Faiq, Nor Afzanizam Samiran, Razlin Abd Rashid, Izuan Amin Ishak, Zuliazura Mohd Salleh, Rais Hanizam Madon, and Muhammad Suhail Sahul Hamid. "Effect of impeller's blade number on the performance of mixing flow in stirred tank using CFD simulation method." *CFD Letters* 14, no. 5 (2022): 33-42. <https://doi.org/10.37934/cfdl.14.5.3342>
- [14] Ahmad, Mohd Nazri, Mohammad Khalid Wahid, Nurul Ain Maidin, Mohd Hidayat Ab Rahman, Mohd Hairizal Osman, Ridhwan Jumaidin, and Muhammad Afiq Abu Hassan. "Flow analysis of five-axis impeller in vacuum casting by computer simulation." *Journal of Advanced Research in Fluid Mechanics and Thermal Sciences* 61, no. 2 (2019): 181-189.
- [15] Grochowalska, Joanna, Piotr Jaworski, and Łukasz Jan Kapusta. "Analysis of the structure of the atomized fuel spray with marine diesel engine injector in the early stage of injection." *Combustion Engines* 195, no. 4 (2023): 97-103. <https://doi.org/10.19206/CE-168394>
- [16] Park, Jung Eun. "Integration of Theory to Computations of Spray and Turbulent Flows." PhD diss., Arizona State University, 2022.
- [17] Lucci, Francesco, Edo Frederix, and Arkadiusz K. Kuczaj. "AeroSolved: Computational fluid dynamics modeling of multispecies aerosol flows with sectional and moment methods." *Journal of Aerosol Science* 159 (2022): 105854. Lucci, Francesco, Edo Frederix, and Arkadiusz K. Kuczaj. "AeroSolved: Computational fluid dynamics modeling of multispecies aerosol flows with sectional and moment methods." *Journal of Aerosol Science* 159 (2022): 105854. <https://doi.org/10.1016/j.jaerosci.2021.105854>

- [18] Ismail, Zurita, Saleha Maarof, Mohamed Faris Laham, Kai Xin Siah, Muhamamd Rezal Kamel Ariffin, and Nizam Tamchek. "CFD Simulation Using ANSYS FLUENT of Jet Nozzle of Ethanol at Temperature of 360 K." *Journal of Advanced Research in Fluid Mechanics and Thermal Sciences* 96, no. 1 (2022): 168-178. <https://doi.org/10.37934/arfmts.96.1.168178>
- [19] Pairan, M. Rasidi, Norzelawati Asmuin, Nurasikin Mat Isa, and Farid Sies. "Characteristic study of flat spray nozzle by using particle image velocimetry (PIV) and ANSYS simulation method." In *AIP Conference Proceedings*, vol. 1831, no. 1. AIP Publishing, 2017. <https://doi.org/10.1063/1.4981150>
- [20] Fazlyyyakhmatov, Marsel, and Linar Shaidullin. "Airflow velocity measurement of the electrostatic spray gun." In *Journal of Physics: Conference Series*, vol. 1588, no. 1, p. 012068. IOP Publishing, 2020. <https://doi.org/10.1088/1742-6596/1588/1/012068>